Polydisperse particle-driven gravity currents propagating into a stratified ambient in containers of general cross sections

T. Zemach [*]

Department of Computer Science, Tel-Hai College, Tel-Hai, Israel

We investigate the behavior of a high-Reynolds-number polydisperse gravity current propagating along a channel of general cross-section form given by a width function $f(z)$ into a linearly stratified ambient fluid of density $\rho_a(z)$. The current of density ρ_c is formed by n types of particles of various densities and settling velocities suspended in an interstitial fluid of density ρ_i. We formulate shallow-water equations of motion and then solve the partial differential equation system of hyperbolic type by the Lax-Wendroff two-step finite-difference method. We present typical profiles for height (h) and velocity (u) of the current and mass concentration (Φ) of the particles. We show that initially the front of the current propagates with an almost constant speed. During the next stage the height and the speed of the nose decrease, which leads to the pseudosimilar final stage of propagation. The solutions are illustrated for flow in typical power-law geometry. The problem introduces two dimensionless parameters: (1) the stratification parameter S ($0 \leqslant S \leqslant 1$), which represents the magnitude of the stratification in the ambient fluid, and (2) the particle buoyancy parameter Π ($\Pi \geqslant 0$). We show that increasing S decreases the velocity of the propagation of the current. The effect of Π is the opposite: as Π increases, the current propagates faster. For a specific dependence between S and Π, an equilibrium is reached for a significant time and the system behaves like a system without particles propagating into the ambient of constant density.

I. INTRODUCTION

Polydisperse particle-driven gravity currents are formed when suspension, created by mixing of particles with different densities and settling velocities with an interstitial fluid, propagates into an ambient fluid due to inherent density differences. During propagation, particles leave the current and settle. Examples of such flows are deep-sea gravity currents, also called turbidity currents. Often, these flows might be responsible for damage of communication cables lying on the bottom of the ocean. An instance of such harm was documented in Taiwan following the Pingtung earthquakes, wherein local fishermen observed disruptions in the waters. Within a few hours, the majority of cables experienced at least one breakage, leading to significant failures in international telecommunications [1].

On the one hand, most of the theoretical and experimental works deal with monodisperse suspension for which the particles forming the current have a uniform settling velocity [2], while in most real situations the particles have different densities, size, and settling velocities. On the other hand, it also has been assumed that the ambient fluid has a constant density, while in many natural situations, especially in the ocean, the ambient is stratified [3]. For example, in shelf seas a themocline may form in <50 m water depth and simultaneously be located close to the seafloor; yet here surface

---

[*]tamar.zemach@yahoo.com

winds and tides may have leading-order control on flow dynamics. However, in deep-water systems (i.e., the Abyssal plain at 4000+ m depth), the pycnocline may be constrained to the top 300 m of the water column, below which density stratification is negligible. Ambient stratification also plays an important role along coastlines, where it influences the occurrence of coastal upwelling events, which bring nutrient-rich deep waters to the surface, fueling productivity in marine ecosystems. The presence of a strong thermocline can inhibit vertical mixing and suppress upwelling, while weaker stratification enhances the likelihood of upwelling. Understanding the interplay among ambient stratification, coastal geography, and wind patterns is essential for predicting the timing and intensity of upwelling events and their ecological impacts.

We also want to point out that the internal stratification of gravity currents might be an important effect. However, it can be effectively ignored due to the dominance of other factors such as topography, sediment volume, or flow dynamics inherent to specific geological or environmental conditions. For example, avalanches, which involve the rapid downhill movement of snow, ice, and debris, often exhibit gravity-current-like behavior. In the case of dry snow avalanches, internal stratification may be limited, with the flow primarily governed by factors such as slope angle, snowpack stability, and the presence of obstacles. While some stratification may occur due to differences in snow density or temperature, it is often secondary to other flow dynamics.

Usually, the behavior of such flows is investigated both experimentally and theoretically in horizontal rectangular containers. Thus, He *et al.* [4] consider monodisperse particle-laden gravity current (GC) propagating into a stratified ambient fluid. The authors develop two- and three-dimensional models and show that the particles may cause a particle-laden current to quickly lose momentum so that the near-constant front velocity of the particle-laden current cannot be maintained if no more particles are resuspended. The works of Mériaux and Kutz-Besson [5,6] present experiments and a simple box model for the bidisperse GC propagating into a constant-density ambient fluid. Additional experiments for the bidisperse GC were presented by Gladstone *et al.* [7]. Harris *et al.* [8] presented a theoretical work for the polydisperse GC spreading into a nonstratified ambient and again this work is limited to containers of rectangular cross section (CS). The problem with such a restriction is that the GCs that spread in a nonrectangular cross-section area such as a triangle, trapezoid, or circle occur more frequently in nature (e.g., rivers) and constructed environments (tunnels, reservoirs, canals).

Additional theoretical work was done by Nasr-Azadani *et al.* [9] and it presents the results of simulations obtained for the mono- and polydisperse GCs interacting with complex bottom topology.

Containers of general CS were also discussed in the literature. A shallow-water (SW) theory for the monodisperse currents is discussed by Zemach [10], who also [11] expands this theory for the polydisperse currents. However, these works were limited to the nonstratified ambients. The work of Zemach *et al.* [12] concentrates on the effect of particles on monodisperse lock-released GCs in stratified and nonstratified ambients in containers of circular and semicircular CSs. This work is based on a previous model of Zemach [10] to formulate the equations of motion for a quite general CS propagating into a linearly stratified ambient. One of the important parameters of the problem is the height ratio of ambient to lock parameter, H. The comparison with the experimental data shows that for the full-depth containers (with the initial depth of the current in the lock being equal to the depth of the ambient fluid) a good match is achieved. However, for the partial-depth case, an adjustment coefficient multiplying the Froude number boundary condition of the speed of the front is needed for a better agreement between the theory and the experiments.

The purpose of the present work is to combine three interesting effects—the polydispersity, stratification, and the general CS geometries—and to investigate the propagation of the finite-volume polydisperse current into a linearly stratified ambient in containers of general CS.

The paper is organized as follows. The SW model is formulated in Sec. II. Section III is dedicated to the finite-difference-method solutions and typical results: the pseudoslumping stage

of propagation is discussed as well as the cases for which the similarity solutions can be derived. An additional simplified box model is formulated and solved in Sec. IV. Finally, in Sec. V we summarize the work and give some conclusions.

II. FORMULATION

We start the formulation with the assumption that a gravity current is a dilute suspension formed by n kinds of small heavy particles of density $\rho_p^{(j)}$, radius $a_p^{(j)}$ ($j = 1, ..., n$), and volume fraction $\kappa^{(j)}(x, z, t)$ [initially $\kappa_0^{(j)}(x, z)$], well mixed with the interstitial fluid of density ρ_i, kinematic viscosity ν, and concentration $(1 - \Sigma_{j=1}^{n} \kappa^{(j)})$. The total concentration of fluid is 1. We start with the dimensional variables. We introduce useful density ratio parameters:

$$\epsilon_b = \frac{\rho_b - \rho_o}{\rho_o}, \quad \epsilon_p^{(j)} = \frac{\rho_p^{(j)} - \rho_i}{\rho_i},$$

$$\epsilon_i = \frac{\rho_i - \rho_o}{\rho_o}, \quad j = 1, \ldots, n. \tag{2.1}$$

From the above, the density of the current can be expressed by

$$\rho_c = \Sigma_{j=1}^{n} \kappa^{(j)} \rho_p^{(j)} + \left(1 - \Sigma_{j=1}^{n} \kappa^{(j)}\right) \rho_i = \rho_i \left[1 + \Sigma_{j=1}^{n} \kappa^{(j)} \epsilon_p^{(j)}\right]. \tag{2.2}$$

The ambient fluid is assumed to be linearly stratified from the density ρ_b at the bottom of the container at $z = 0$ to the density ρ_o at its top at $z = H$ (we assume that $0 \leqslant z \leqslant H$) and to have the density

$$\rho_a(z) = (\rho_o - \rho_b)\frac{z}{H} + \rho_b, \tag{2.3}$$

where the density of the interstitial fluid is larger than or equal to the density of the ambient at the bottom: $\rho_i \geqslant \rho_b$. For an ambient stratified fluid, we define a buoyancy frequency by

$$\mathcal{N}^2 = -\frac{g}{\rho_o}\frac{d\rho_a}{dz}. \tag{2.4}$$

We employ Cartesian coordinates $\{x, y, z\}$ with corresponding $\{u, v, w\}$ velocity components. Initially, a suspension of height h_0 and length x_0 is located at rest ($u = v = w = 0$) in a horizontal container of height H (see Fig. 1). The sidewalls of the reservoir are uniform in the x direction, where the CS is described by the functions $y = -f_1(z)$ and $y = f_2(z)$, which define the width of the reservoir to be $f(z) = f_1(z) + f_2(z)$ [13]. At $t = 0$ a fixed volume of denser-than-ambient fluid is instantaneously released into the ambient fluid. For the ambient fluid we assume that $u_a = v_a = w_a = 0$ during all stages of the current's propagation. We neglect the effects of viscosity, turbulence, and entrainment and assume that the domain of the current and of the ambient are separated by a sharp and flat interface in the y direction. We also note that the channel of arbitrary cross section has some inherent stratification within it that is of similar scale to the depth of the gravity current. All these simplifications do not affect the correctness of the results in many practical situations; this is true even for more simplified models (see Ref. [14], where a box model favorably compares with the experiments).

Additional notations and assumptions are as follows: (1) $h(x, t)$ is the thickness of the current, initially $h = h_0$; (2) the current is shallow with $h_0/x_0 \ll 1$; (3) $u(x, t)$ is the velocity of the current, averaged over the area of the current, initially $u = 0$; (4) the variable $\kappa(x, t)$ is also averaged over the area of the current; (5) we assume a Boussinesq approximation ($\frac{\rho_i}{\rho_o} \approx 1$); and (6) the Reynolds number gives an indication of the ratio of two effects: inertial and viscous effects. Here we assume that the current is in the inviscid or inertial regime and the Reynolds number is large and is defined by $\mathrm{Re} = h_N u_N / \nu$. (7) Turbulent remixing is assumed: all the fluid of the initial current remains as part
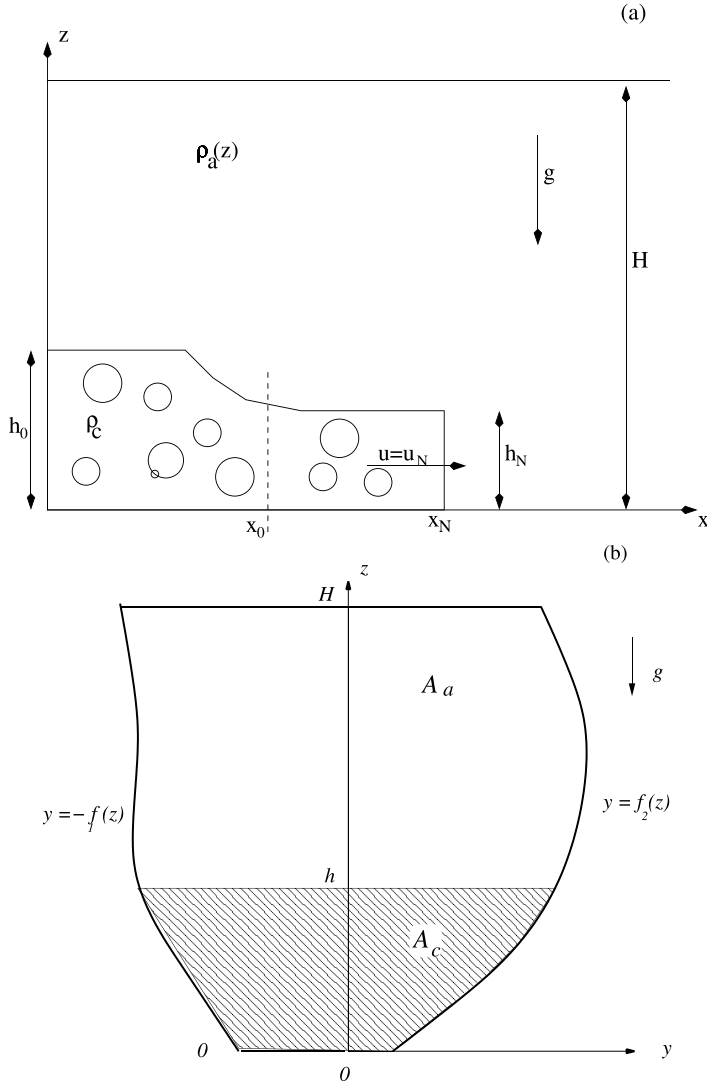
(a)

(b)

FIG. 1. Schematic description of the current released from a lock of length x_0 and height h_0 in the channel of height H with nonrectangular cross section: (a) Side view. (b) Cross section of channel. Here $f(z) = f_1(z) + f_2(z)$ is the width of the channel. In the analysis A_a denotes the area occupied by the ambient fluid, A_c is the area occupied by the current, and $A_T = A_c + A_a$ is the total area.

of the current in the domain $0 \leqslant z \leqslant h(x, t)$. The dispersed particles settle out from the current only at the bottom, with constant velocity calculated from the Stokes formula. The remaining nonsettled particles are remixed vertically in the current so that the volume fraction is homogeneous over the cross section. At the interface $z = h(x, t)$, there is no relative motion between the current and the particles.

Next, we use the subscripts c and a to denote the current and the ambient domains and define the CS of the current as $A_c = A(h) = \int_0^h f(z)dz$ and the total CS of the channel as $A_T = \int_0^H f(z)dz$.

Now we develop the expressions for the pressures in both the ambient and the current domains, under the assumption that the pressures satisfy the hydrostatic balance and the continuity condition

$p_c = p_a = \text{const}$ at the interface $z = h(x, t)$. Thus,

$$p_a(x, z, t) = -g\rho_o z\Big[1 + \epsilon_b\Big(1 - \frac{z}{2H}\Big)\Big], \tag{2.5}$$

$$p_c(x, z, t) = g\rho_i\big[1 + \Sigma_{j=1}^n \kappa^{(j)}\epsilon_p^{(j)}\big](h - z) + p_a(h), \tag{2.6}$$

and so the pressure gradient in the current can be expressed by

$$\frac{\partial p_c}{\partial x} = g\rho_i\Bigg[\big(h\big(1 + \Sigma_{j=1}^n \kappa^{(j)}\epsilon_p^{(j)}\big)\big)_x - z\big(\Sigma_{j=1}^n \kappa^{(j)}\epsilon_p^{(j)}\big)_x - \frac{\partial h}{\partial x}\Big(1 + \epsilon_b\Big[1 - \frac{h}{H}\Big]\Big)\Bigg]. \tag{2.7}$$

We introduce

$$\Sigma = \Sigma_{j=1}^n \kappa^{(j)}\epsilon_p^{(j)}, \tag{2.8}$$

$$\Sigma_0 = \Sigma_{j=1}^n \kappa_0^{(j)}\epsilon_p^{(j)}, \tag{2.9}$$

the dimensionless stratification parameter

$$S = \frac{\epsilon_b}{\epsilon_i} = \frac{\rho_b - \rho_o}{\rho_i - \rho_o}, \tag{2.10}$$

and the dimensionless particle buoyancy parameter

$$\Pi = \frac{\Sigma_0}{\epsilon_i} = \Sigma_{j=1}^N \kappa_0^{(j)} \frac{\epsilon_p^{(j)}}{\epsilon_i}, \tag{2.11}$$

which compares the effect of particles' presence in the current to the stratification of the ambient fluid and is assumed to be positive. We note that for hyperpycnal flows Π is strictly positive, since $\rho_p > \rho_i$ and $\rho_i > \rho_o$. But for lofting flows this may not be the case.

Now we move to the dimensionless variables defined as follows (here the dimensional variables are denoted by an asterisk):

$$\{x^*, z^*, h^*, H^*, t^*, u^*, p^*\} = \{x_0 x, h_0 z, h_0 h, h_0 H, T t, U u, \rho_o U^2 p\}, \tag{2.12}$$

where $U = (g\epsilon_i h_0)^{1/2}$ and $T = x_0/U$. In addition, we employ the scaled mass fraction variables (here $j = 1, \ldots, n$),

$$\phi^{(j)} = \frac{\kappa^{(j)}\epsilon_p^{(j)}}{\Sigma_{m=1}^n \kappa_0^{(m)}\epsilon_p^{(m)}}, \tag{2.13}$$

which are in the range [0, 1]. Initially, $\phi^{(j)}(x, 0) = \phi_0^{(j)}$, where $\Sigma_{j=1}^n \phi_0^{(j)} = 1$.

The settling speed of a particle, which is assumed to be small, can be calculated from the Stokes formula by

$$W_s^{(j)} = \frac{2}{9}\epsilon_p^{(j)} \frac{\big(a_p^{(j)}\big)^2}{\nu} g. \tag{2.14}$$

Additional dimensionless parameters are $\beta^{(j)} \ll 1$ ($j = 1, \ldots, n$), which are defined by the ratio between the propagation time of the current for a distance x_0 to the particle settling time for a height h_0:

$$\beta^{(j)} = \frac{W_s^{(j)}}{U} \frac{x_0}{h_0}. \tag{2.15}$$

A. The governing equations

The system of $n + 2$ governing equations of motion can be written in the region of the current in terms of h, u, $\phi^{(j)}$ ($j = 1, ..., n$) or, alternatively, in conservation forms in terms of $A(h)$, $uA(h)$, and

$\phi^{(j)}A(h)$. However, the following transformation (see Ref. [11] and Appendix for details),

$$\phi^{(j)}(x, t) = \phi_0^{(j)} e^{\beta^{(j)} G(x,t)}, \tag{2.16}$$

[initially $G(x, 0) = 0$] reduces this system of $n + 2$ equations to a system of three equations only, written in conservation form in terms of $A(h)$, $uA(h)$, and $GA(h)$:

$$\frac{\partial A}{\partial t} + \frac{\partial (Au)}{\partial x} = 0,$$

$$\frac{\partial (Au)}{\partial t} + \frac{\partial (Au^2)}{\partial x} + \frac{\partial A}{\partial x} \frac{A}{f(h)} \left[\Pi\Phi + 1 - S\left(1 - \frac{h}{H}\right) \right] + \Pi\frac{\partial \Phi}{\partial x} A\Psi(h) = 0,$$

$$\frac{\partial (AG)}{\partial t} + \frac{\partial (AGu)}{\partial x} = -f_M, \tag{2.17}$$

where

$$\Psi(h) = h - \frac{\int_0^h zf(z)dz}{\int_0^h f(z)dz}, \tag{2.18}$$

$$f_M(h) = \max\left(f(h), f(0)\right), \tag{2.19}$$

and

$$\Phi = \Phi(x, t) = \Sigma_{j=1}^n \phi^{(j)}(x, t) = \Sigma_{j=1}^n \phi_0^{(j)} e^{\beta(j)G(x,t)}, \quad \text{with} \quad \Phi(x, 0) = 1. \tag{2.20}$$

The equations can also be rewritten in the characteristic form:

$$\begin{pmatrix} h \\ u \\ G \end{pmatrix}_t + \begin{pmatrix} u & \frac{A}{f(h)} & 0 \\ \Lambda & u & \Pi\Psi^*(h) \\ 0 & 0 & u \end{pmatrix} \begin{pmatrix} h \\ u \\ G \end{pmatrix}_x = \begin{pmatrix} 0 \\ 0 \\ -\frac{f_M(h)}{A(h)} \end{pmatrix}, \tag{2.21}$$

where

$$\Psi^* = \Psi\Sigma_{j=1}^n \phi_0^{(j)} \beta^{(j)} e^{\beta^{(j)}G(x,t)} \tag{2.22}$$

and

$$\Lambda = \Pi\Phi + 1 - S\left(1 - \frac{h}{H}\right). \tag{2.23}$$

System (2.21) is hyperbolic and it provides the following relationships on the characteristics:

$$dh \pm \sqrt{\frac{A}{f(h)} \frac{1}{\Lambda}} du + \frac{\Pi\Psi^*}{\Lambda} dG = -\frac{\Pi\Psi^*}{\Lambda} \frac{f_M(h)}{A(h)} dt \quad \text{on} \quad \frac{dx}{dt} = u \pm \sqrt{\Lambda\frac{A(h)}{f(h)}} \tag{2.24}$$

and

$$dG = -\frac{f_M(h)}{A(h)} dt \quad \text{on} \quad \frac{dx}{dt} = u. \tag{2.25}$$

B. Initial and boundary conditions

Initially, in the domain of the current ($0 \leqslant x \leqslant 1$), $u = 0$, $h = 1$, $G = 0$, and $\Phi = 1$. An additional boundary condition is $u = 0$ at $x = 0$.

The presence of the stratification and the particles is expected to reduce the speed of the propagation, u_N [2,15]. Here the subscript N denotes values associated with the "nose" of the current. Indeed, at early times the particle-driven currents are the same as the equivalent homogeneous currents because very few particles have settled out of the suspension. At later times, the lengths of the particle-driven currents are less than their homogeneous counterparts because the loss of

particles reduces the buoyancy driving force at the nose. During the propagation, the stratification also reduces the effective driving force and, hence, the inertial effects.

Unfortunately, a rigorous extension of the formula of u_N for these effects is not available. Therefore, we follow here the approximate method used for stratified currents in general geometries [16].

At the nose $x = x_N$, the boundary condition for u_N in dimensional form can be approximated by

$$u_N = (g\epsilon_i)^{1/2} \Upsilon^{1/2} h_N^{1/2} \text{Fr}(a). \tag{2.26}$$

In dimensionless form it becomes

$$u_N = \Upsilon^{1/2} h_N^{1/2} \text{Fr}(a), \tag{2.27}$$

where $a = h_N/H$ and $\text{Fr}(a)$ is a Froude number function [11,17]:

$$\text{Fr}(a) = \text{Fr}(\varphi) = \left[\frac{2(1-\varphi)^2}{1+\varphi}(1+Q) \right]^{1/2}, \tag{2.28}$$

where

$$\varphi = \frac{A}{A_T} \quad \text{and} \quad Q = \frac{\int_0^h zf(z)dz}{h[A_T - A]}. \tag{2.29}$$

The slow-down coefficient Υ is the ratio of the pressure force over the nose in the presence of the stratification and the particles to the pressure force when no particles and no stratification are present ($S = 0, \Pi = 0$):

$$\Upsilon = \frac{\int_0^{h_N} (p_c - p_a)_{(S,\Pi)} f(z)dz}{\int_0^{h_N} (p_c - p_a)_{(S=0,\Pi=0)} f(z)dz}. \tag{2.30}$$

Substitution of the pressures in Eqs. (2.5) and (2.6) provides a more explicit form of the coefficient Υ:

$$\Upsilon = 1 + \Pi\Phi - S\left[1 - \frac{1}{2}\frac{h_N}{H}(1+\gamma) \right], \tag{2.31}$$

where

$$\gamma = \frac{\int_0^{h_N} z/h_N(h_N - z)f(z)dz}{\int_0^{h_N} (h_N - z)f(z)dz}. \tag{2.32}$$

We also mention that the dimensionless speed of the fastest mode internal wave in the ambient fluid is (see Ref. [15]) $u_W = \frac{(SH)^{1/2}}{\pi}$. A current is defined as supercritical when $u_N > u_W$ and subcritical when $u_N < u_W$. Theory and experiments show that both supercritical and subcritical currents are feasible. Coupling the front speed and the internal waves in order to understand the effects of the interaction requires a more sophisticated model than the simple one used here. Indeed, a major deficiency of the one-layer SW model is that the internal gravity waves in the stratified ambient are discarded. When the propagation is with subcritical speed, a wave-nose interaction appears after some propagation. These interactions can lead to the slowing down of the current, potentially compromising the accuracy of subsequent predictions made by the SW model. While a thorough discussion of these complex interactions is not within the scope of the present paper, interested readers are directed to further explore the topic in Ungarish's work [15] and the related literature therein.

C. Preliminary model validation

It is essential to verify the model using various simpler cases before implementing the current approach.

(1) For general $f(z)$, $\beta^{(1)} \neq 0$, $\beta^{(j)} = 0$, $j = 2, \ldots, n$, and $S \neq 0$, the model reduces to the formulation of monodisperse particle-driven gravity currents propagating in a stratified ambient. The equations and the boundary conditions for this case were formulated by Zemach *et al.* [12] and validated experimentally in containers of circular and semicircular CSs [$f(z) = 2\sqrt{2Rz - z^2}$, where R is the radius of the container]. Zemach *et al.'s* results show good agreement between the SW results and the experimental data for the full-depth ($H = 1$) cases for various values of S. However, for the partial-depth cases ($H > 1$), they suggest using a Froude correction coefficient $\chi < 1$ (in most experiments $\chi \in [0.7, 0.8]$) to reproduce a better comparison with the numerical results.

(2) For $\Pi = 0$ (or $\beta^{(j)} = 0$, $j = 1, \ldots, n$) and for a given general CS function $f(z)$, the model becomes identical to the theory of homogeneous gravity currents propagating in the stratified ambient [16].

(3) For $S \to 0$, the formulation can be reduced to the propagation of a polydisperse GC in homogeneous ambient, discussed by Zemach [11] for $\Pi \gg 1$. The reason is as follows: as $S \to 0$, it can be concluded from Eqs. (2.27)–(2.31) that, for a significant propagation of the current, Π should be large. Thus, the present formulation convergences to the previous theory [11]. The qualitative and quantitative behavior of the polydisperse current obtained from the theory was supported by the results provided by previous experiments [5,6].

III. RESULTS FOR GENERAL $f(z)$

To solve the system of equations (2.21) with corresponding initial and boundary conditions (2.27)–(2.29), we employ a two-step Lax-Wendroff finite-difference numerical method. We first transfer the original x coordinate to $\eta = x/x_N(t)$, so the domain of the solution remains constant ($0 \leqslant \eta \leqslant 1$). Next, we run the code using 200 grid points in the $[0, x_N]$ interval with a time step of 1×10^{-3} for different sets of free parameters (H, $f(z)$, $\beta^{(j)}$ ($j = 1, \ldots, n$); $\phi_0^{(j)}$ ($j = 1, \ldots, n$); Π and S) to obtain the height, velocity, and distance of propagation of the current as well as the concentrations of the particles.

A. Pseudoslumping stage

The classical initial slumping stage of propagation is characterized by a constant height h_N and speed u_N of the nose. We note that the balances of the characteristics (2.24) obtained by analytical methods are complicated by the time-dependent term, and the boundary condition (2.27) at $x = x_N$ is also time dependent. Therefore, a simple analytical solution for the slumping stage is not available. To understand the nature of this stage, we employ the finite-difference solution.

Figure 2 shows typical solutions for the height of the nose, h_N, the speed of the nose, u_N, and the distance of propagation, x_N, as function of t in containers of parabolic form [$f(z) = z^2$] for $H = 2$, $S = 0.5$, and various values of $\Pi = 0, 0.5, 1.0$. The polydisperse phase is bidisperse and it consists of two types of particles with $\beta^{(1)} = 0.0025$, $\phi^{(1)} = 0.8$; $\beta^{(2)} = \beta^{(1)}/7 = 0.00036$, $\phi^{(2)} = 0.2$, correspondingly.

Initially, the nose propagates with constant height h_N. The differences between the slumping height h_N are not significant for various values of Π. After the slumping period, the nose height h_N decreases and the slumping distance $x_N^{(s)}$ becomes shorter as Π increases. Thus, for $\Pi = 0$, the slumping finishes at $t \approx 12.5$, while for $\Pi = 1$, the slumping is over much earlier, at about $t \approx 8$. The velocity of the nose during the slumping phase depends on Π: it increases with Π and approaches its minimum for $\Pi = 0$. But the interesting thing is that the speed of the nose is not exactly constant during this period. Indeed, as we can see, for $\Pi = 0$, the speed u_N is constant during the entire slumping stage ($u_N \approx 0.8$). However, for $\Pi > 0$, the speed of the nose slightly decreases during the entire slumping stage (which should be called now the pseudoslumping stage). The decrease of u_N is about 5%. Such behavior, observed for the polydisperse system, was also noted for the monodisperse currents propagating in nonstratified [18] and stratified ambient [4]. In particular, we could anticipate that a particle-driven current loses particles (i.e., driving force) during
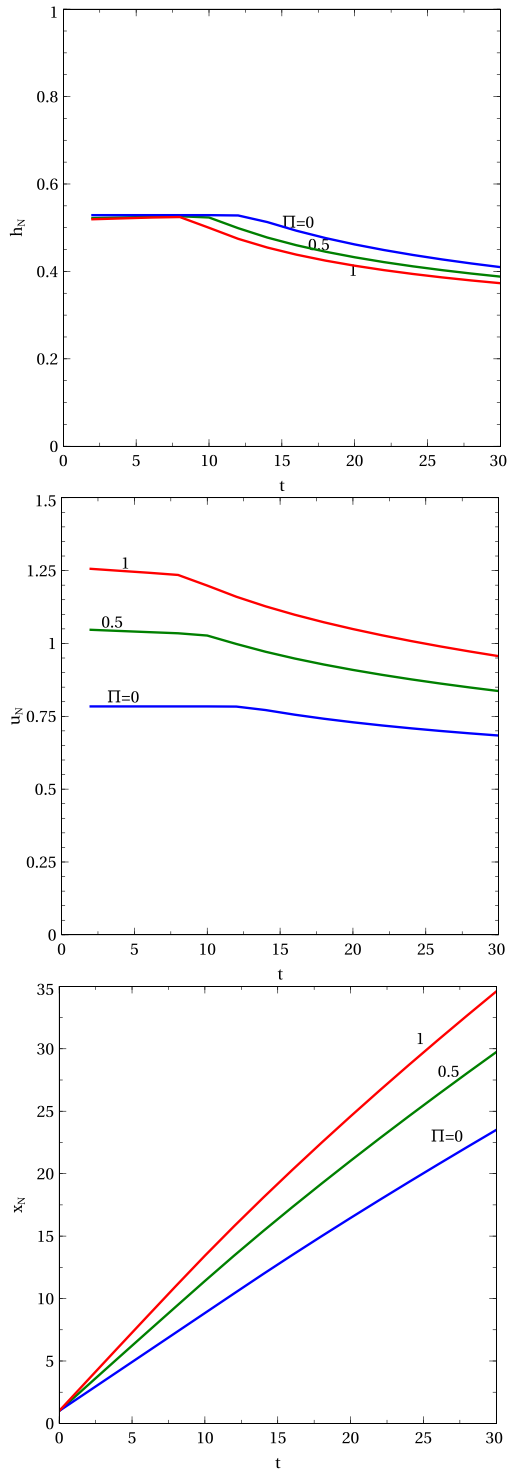
FIG. 2. Pseudoslumping stage in container of parabolic CS with $f(z) = z^2$ and $H = 2$. Here $S = 0.5$ and $\Pi = 0, 0.5, 1.0$. The current is bidisperse with $\beta^{(1)} = 0.0025$, $\phi^{(1)} = 0.8$; $\beta^{(2)} = \beta^{(1)}/7 = 0.00036$, $\phi^{(2)} = 0.2$.

the motion so that a constant front velocity of the particle-driven current cannot be maintained. Mathematically, such behavior can be explained by the analysis of the balances of the characteristics in Eqs. (2.24). Indeed, Eqs. (2.24) depend on time t (the term multiplied by dt), which means that velocity of the current u and its h are not expected to be constant also during the initial stages of propagation. On the other hand, since the settling is slow, the decrease of u_N is mild.

Additional results are shown for fixed value of $\Pi = 0.5$ and various values of $S = 0.01, 0.5, 0.75, 1.0$ in Fig. 3. Other parameters of the problem are identical to those described above for Fig. 2. As we can see, as S increases, the slumping height h_N increases and the slumping becomes longer. The speed of the nose, u_N, decreases slightly during this stage. As S increases, u_N becomes smaller.

Figure 4 shows additional results obtained for a parabolic container of different height $H = 20$ and quadridisperse phase, which consists of four types of particles with $\beta^{(1)} = 0.0175, \phi^{(1)} = 0.2; \beta^{(2)} = 0.0025, \phi^{(2)} = 0.3; \beta^{(3)} = 0.00036, \phi^{(3)} = 0.3; \beta^{(4)} = 0.0000514; \phi^{(4)} = 0.2$. Here $\Pi = 0.5, S = 0.01, 0.5, 1.0$. The effects of S and Π in this system are similar to those discussed above in the context of bidisperse systems.

B. The time-dependent flow

The typical behavior of the current propagating into the stratified ambient fluid is shown as an example of bidisperse current spreading in a channel of parabolic CS [$f(z) = z^2$] with $H = 2$ into a stratified ambient. The profiles are shown in Fig. 5. Here $\beta^{(1)} = 2.5 \times 10^{-3}$ and $\phi^{(1)} = 0.8$, $\beta^{(1)}/\beta^{(2)} = 7, \phi^{(2)} = 0.2$, and $S = \Pi = 0.5$.

The initial stage of propagation is the pseudoslumping stage. The next stage is characterized by the decreasing height of the nose and the speed. This stage is a transition to the last pseudosimilarity stage. The transition is smooth and it is therefore not possible to give a clear-cut statement regarding when this intermediary phase ends. The long-time profiles display a tendency to pseudo-self-similar behavior, which can be identified by a "tail-down–nose-up" form of height h.

Figures 2 and 3 show the distance of propagation, x_N, as a function of time t for various combinations of S and Π. For a fixed value of Π, x_N decreases when S increases. Such behavior was also obtained for the homogeneous currents (see Ref. [18]) and is expected according to Eqs. (2.27) and (2.31). Indeed, as S increases, Υ decreases and so does u_N. The effect of Π is the opposite: x_N increases as Π increases. This again can be explained using the front conditions (2.27) and (2.31).

From the graphs and the analysis of the equations we can see that the effects of both the stratification of the ambient and the presence of the particles in the current are actually independent when $S > 0$ and $0 \leqslant \Pi \leqslant 1$ and can be analyzed separately. The effect of the stratification vanishes when $\Pi \gg 1$. Indeed, for quite large values of Π (say, $\Pi > 5$), according to Eqs. (2.23) and (2.31), the term $(1 + \Pi\Phi)$ becomes dominant and so the stratification almost does not effect the system. In such cases, the system becomes (almost) identical to one with a nonstratified ambient. For $\Pi \to 0$, only the effect of stratification is important and the current becomes homogeneous.

We recall that the nose boundary condition is given by Eqs. (2.27)–(2.31). For $\Pi = 0$ and $S = 0$, $\Upsilon = 1$ and boundary condition (2.27) becomes the classical boundary condition for the nonparticles, nonstratified ambient case. Above we mentioned that, on the one hand, the increasing values of the parameter of particles, Π, increase the velocity of propagation of the current. However, on the other hand, increasing of the stratification parameter S decreases the speed of the current. Thus, if $\Pi \approx \frac{1}{S}(1 - \frac{1}{2H})$, then $\Upsilon \approx 1$ and the particle-driven current is also expected to behave like a homogeneous GC in a nonstratified ambient. Indeed, this condition shows a particular case for which the presence of the particles in the current is counteracted by the presence of the stratification in the ambient. In this case the current behaves for a significant time period like one without particles and without the stratification in the ambient. Figure 6 compares between the homogeneous GC spreading in the nonstratified ambient with polydisperse GC ($\beta_1 = 0.0025$ and $\phi_1 = 0.8; \beta_2 = 0.00036$ and $\phi_2 = 0.2$) propagating into an ambient fluid with $S = 0.8$. Here $H = 20$ and we chose the value of Π to be equal to $\Pi \approx \frac{1}{S}(1 - \frac{1}{2H}) \approx 1.219$. As we can see, the agreement is good with discrepancy
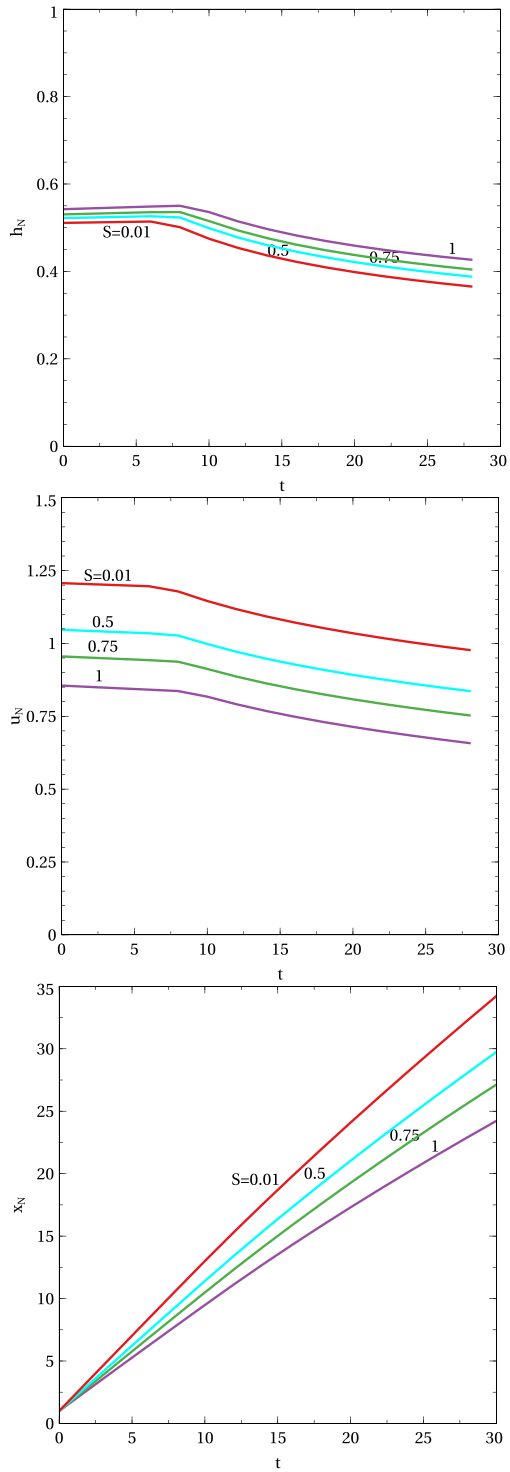
FIG. 3. Pseudoslumping stage in container of parabolic CS with $f(z) = z^2$ and $H = 2$. Here $\Pi = 0.5$; $S = 0.01, 0.5, 0.75, 1.0$. The current is bidisperse with $\beta^{(1)} = 0.0025$, $\phi^{(1)} = 0.8$; $\beta^{(2)} = \beta^{(1)}/7 = 0.00036$, $\phi^{(2)} = 0.2$.
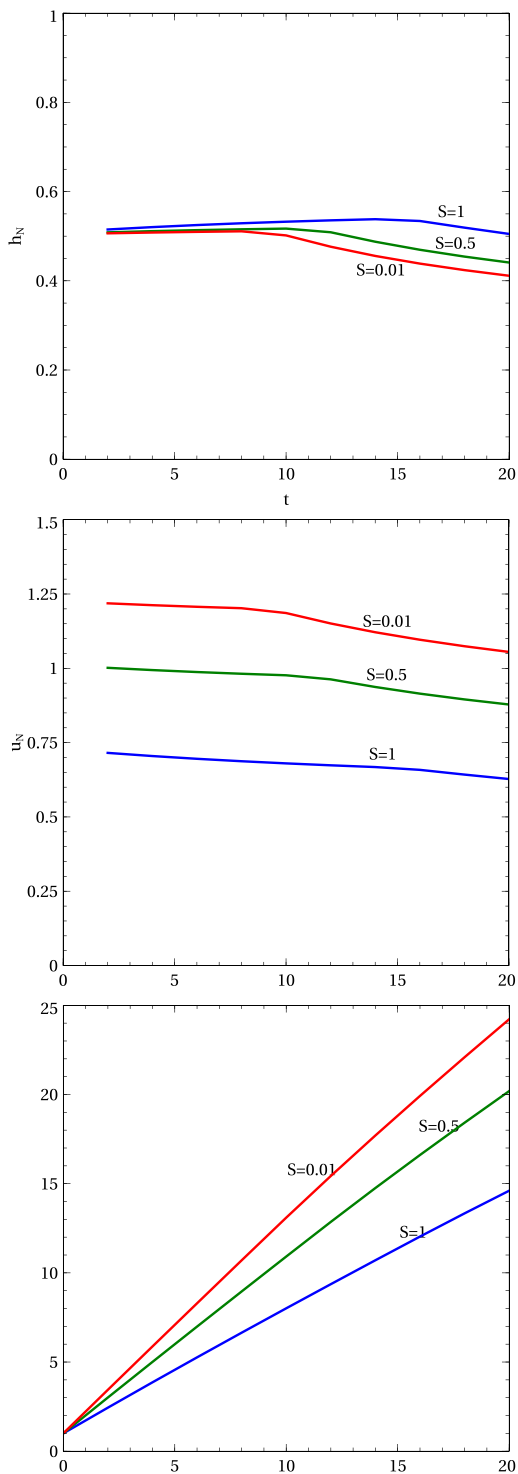
FIG. 4. Pseudoslumping stage in container of parabolic CS with $f(z) = z^2$ and $H = 20$. Here $\Pi = 0.5$; $S = 0.01, 0.5, 1.0$. The current is quadridisperse with $\beta^{(1)} = 0.0175$, $\phi^{(1)} = 0.2$; $\beta^{(2)} = 0.0025$, $\phi^{(2)} = 0.3$; $\beta^{(3)} = 0.00036$, $\phi^{(3)} = 0.3$; $\beta^{(4)} = 0.0000514$; $\phi^{(4)} = 0.2$.
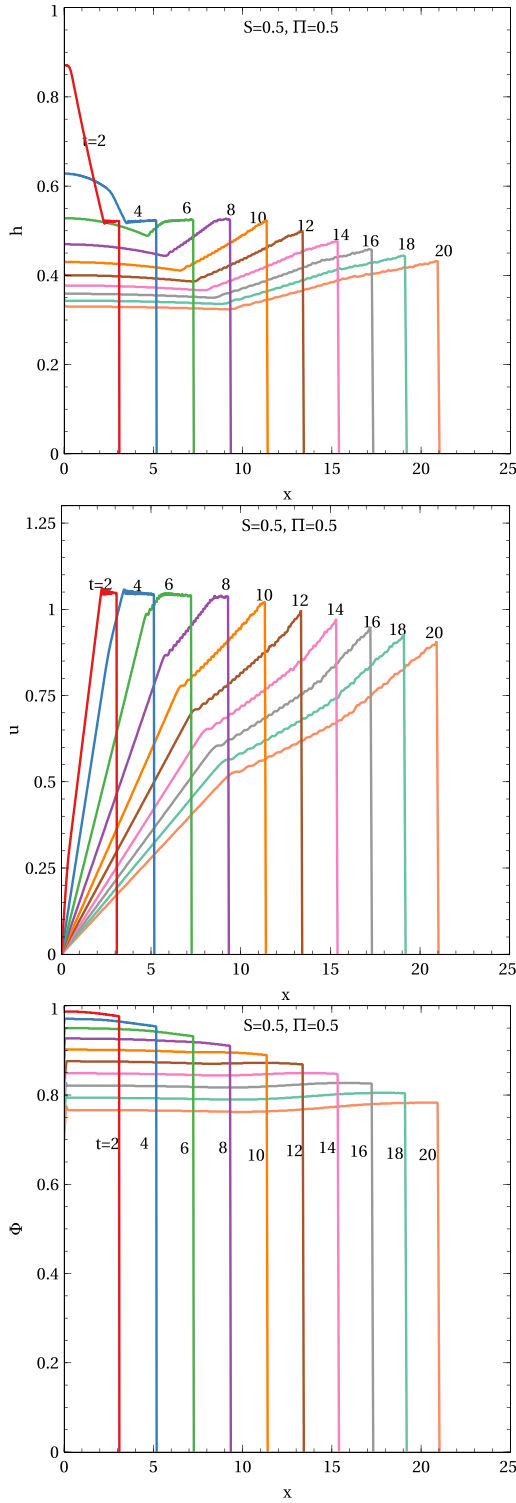
FIG. 5. Profiles for parabolic CS $f(z) = z^2$. $S = 0.5$, $\Pi = 0.5$. Bidisperse with $\beta^{(1)} = 0.0025$, $\phi^{(1)} = 0.8$; $\beta^{(2)} = \beta^{(1)}/7 = 0.0036$, $\phi^{(2)} = 0.2$. $H = 2$.
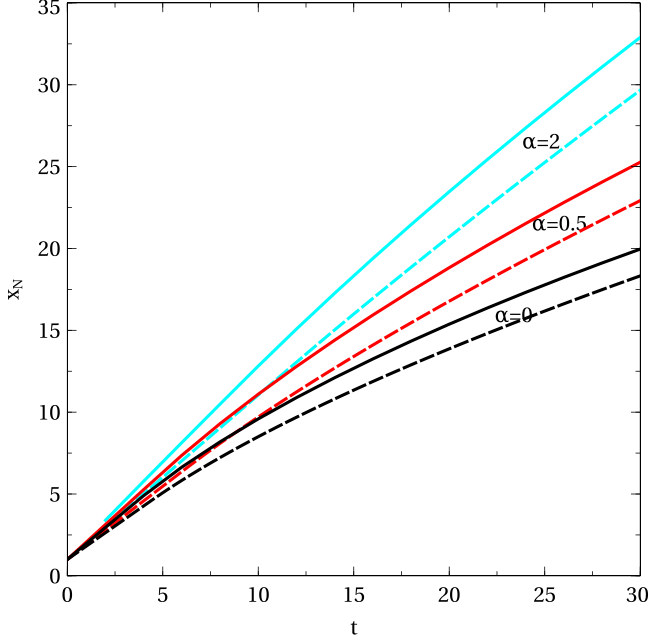
FIG. 6. Bidisperse GC (solid line) with $S = 0.8$ and $\Pi \approx \frac{1}{S}(1 - \frac{1}{2H}) \approx 1.219$ vs GC with no particles and nonstratified ambient (dashed line). Here $f(z) = z^\alpha$ with $\alpha = 0, 0.5, 2$ and $H = 20$.

of less than 10% even for quite progressive times for all the examined values $\alpha = 0, 0.5, 2$. The comparison between the profiles of h and u (not shown here) provides a similar agreement.

1. Monodisperse current of average settling velocity

The suspended particles in natural and environmental particle-driven GCs do not have equal settling velocities. However, it may be convenient to approximate such polydisperse systems by a monodisperse system with one type of particle of average settling velocity $\overline{\beta}$, defined by

$$\overline{\beta} = \Sigma_{j=1}^n \beta^{(j)} \phi_0^{(j)}. \tag{3.1}$$

In the case of nonstratified ambients [8,11] it was found that a polydisperse current behaves like a monodisperse current of average settling velocity when

$$\Sigma_{j=1}^n \left(\frac{\beta^{(j)}}{\overline{\beta}} - 1 \right)^2 \phi_0^{(j)} \ll 1, \tag{3.2}$$

which means that the distribution of the polydisperse system is very narrow.

A comparison between the polydisperse and corresponding monodisperse systems with stratified ambient leads to a similar conclusion. In particular, for various values of $S = 0.001, 0.5$ and $\Pi = 0.5, 1$ we compared (1) the bidisperse cases described above ($\beta^{(1)} = 0.0025, \phi^{(1)} = 0.8; \beta^{(2)} = 0.00036, \phi^{(2)} = 0.2$) with the monodisperse case ($\overline{\beta} = 0.0021$) and (2) the quadridisperse cases

$$(\beta^{(1)} = 0.0175, \quad \phi^{(1)} = 0.2; \quad \beta^{(2)} = 0.0025, \quad \phi^{(2)} = 0.3;$$
$$\beta^{(3)} = 0.00036, \quad \phi^{(3)} = 0.3; \quad \beta^{(4)} = 0.0000514; \quad \phi^{(4)} = 0.2.$$

with the monodisperse case ($\overline{\beta} = 0.00437$) and found that the solutions of $x_N(t)$ differ very slightly for small values of $\beta^{(j)}$.

C. Similarity solution

In general, no similarity solution can be obtained for the systems discussed. In particular, no solutions are known even for the monodisperse GC propagating in the rectangular container. Some works suggest approximate similarity solutions for the monodisperse particle-driven currents propagating into the nonstratified ambient in containers of rectangular CS [19] and of power-law CSs [20]. No similarity solutions are also known for the homogeneous GC propagating into the stratified fluid, except for one particular case with $S = 1, \Pi = 0$. Such a special case was discussed by Ungarish [16] and was restricted for the containers of rectangular or power-law CSs only. The main reason why the similarity solution is not available for the present configuration is the special structure of boundary condition (2.27), which involves parameters that are not given to separation as multiplied factors and therefore the usual assumption regarding the form of the similarity solution cannot be made.

IV. BOX MODEL

In this section we provide a major generalization of the box model for polydisperse currents propagating in channels of rectangular or power-law CSs.

We must keep in mind that in spite of its formal simplicity, the box model does not reproduce the inner behavior of the currents and so using the SW approach is much more accurate. The main advantage of the box model is that it has been used for quick estimates of the global behavior of the gravity currents (see Ref. [15]). Additional advantages and deficiencies were discussed widely concerning homogeneous ($\beta = 0$) [13], monodisperse [10,21], and polydisperse currents [8].

The motion is governed by the total mass conservation and a Froude front condition. The current is assumed to be a "box" of uniform area $A(h(t))$ [evidently, $h = h_N(t)$] and length $x_N(t)$ whose total volume V is constant:

$$V = A(h)x_N. \tag{4.1}$$

The nose condition (2.27) is

$$\frac{dx_N}{dt} = \Upsilon^{1/2}h^{1/2}\text{Fr}, \tag{4.2}$$

where Υ is given by Eq. (2.31). Using Eq. (4.1), we eliminate $x_N = \frac{V}{A(h)}$ to obtain

$$\frac{dx_N}{dt} = -V\frac{f(h)}{A(h)^2}\frac{dh}{dt}. \tag{4.3}$$

Substitution of Eq. (4.3) into boundary condition (4.2) yields

$$\frac{dh}{dt} = -\frac{1}{V}\frac{A^2}{f}\text{Fr}(h)h^{1/2}\Upsilon^{1/2}. \tag{4.4}$$

In the spirit of the box-model simplifications, we also assume that the distribution of the particles depends only on t and not on x. This implies $G = G(t)$ and the use of the last of Eqs. (2.21) gives

$$\frac{dG}{dt} = -\frac{f_M}{A}. \tag{4.5}$$

The combination of Eqs. (4.4) and (4.5) provides the system of nonlinear ordinary differential equations (4.4) and (4.5), which can be integrated by a standard numerical method under the initial conditions $h(0) = 1, G(0) = 0$ to provide $h(t)$ and $G(t)$. Then substitution of $h(t)$ into Eq. (4.1) provides $x_N(t)$.

The analytical calculation of $x_N(t)$ is straightforward only for power-law containers with $f(z) = z^\alpha$ with specific stratification $S = 1$ only and no particles ($\Pi = 0$). Such a case was discussed by Ungarish [16]. Figure 7 shows a comparison between the SW and box-model (BM) solutions for
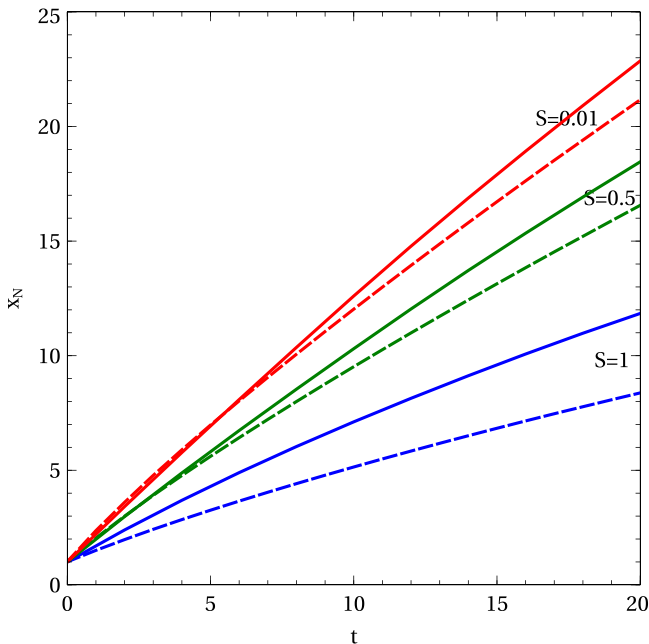
FIG. 7. Comparison between SW (solid) and BM (dashed) solutions in containers of parabolic CS, $f(z) = z^2$. $S = 0.01, 0.5, 1; \Pi = 0.5$. The GC is bidisperse with $\beta^{(1)} = 0.025, \phi^{(1)} = 0.8; \beta^{(2)} = \beta^{(1)}/7 = 0.0036, \phi^{(2)} = 0.2$.

the $H = 20$ case in containers of parabolic form $[f(z) = z^2]$ and bidisperse current with $\beta^{(1)} = 0.025, \phi^{(1)} = 0.8, \beta^{(2)} = 0.0036, \phi^{(2)} = 0.2$. Here $\Pi = 0.5$ and various values of S are used: $S = 0.01, 0.5, 1.0$. Comparison between the BM and SW shows that the SW predicts a faster propagation of the current. Thus, for small values of S, for progressive times the BM solution differs from the SW by 10%. As S grows, the deviation increases. For $S = 0.5$ the difference is about 12% at $t = 20$. However, as S approaches a value of 1, we can see that the differences between the solutions approach about 30% at $t = 20$.

V. SUMMARY AND CONCLUSIONS

In this study we have developed a theoretical model for gravity current flows driven by a polydisperse suspension of particles into a linearly stratified ambient in channels of general CSs. The SW equations of motion were formulated from first principles for three variables only: the height of the current, h, the area-averaged current velocity, u, and the modified function of concentration mass fraction, G. The importance of the particles in the current is expressed by the parameter Π ($\Pi \geqslant 0$), while the parameter S ($0 \leqslant S \leqslant 1$) indicates the importance of the stratification of the ambient. Additional parameters of the problem are the initial concentrations and settling velocities of the particles; the height of the ambient, H, and the geometry of the container, $f(z)$. We wish to emphasize the generality of the approach: it covers various CSs (power law, circular, and trapezoidal), various combinations of particles and interstitial fluid, and various stratifications of the ambient.

To solve the SW problem, we employed a simple Lax-Wendroff two-step finite-difference method, which provides the numerical solutions within an insignificant computational effort on a simple laptop computer.

Three main stages of propagation were determined. The first pseudoslumping stage is characterized by an almost constant speed of propagation u_N for $\Pi > 0$. However, no real slumping (with

constant u_N) was observed, since for $\Pi > 0$, when the particles settle out from the current, the velocity of the nose, u_N, decreases constantly during the initial stage. Next comes the transitional stage and then, only for $\Pi = 0$ and $S = 0, 1$, a similarity solution can be obtained.

Additional effects of the governing parameters of the problem are as follows:

(1) For the homogeneous currents, the stratification ($S > 0$) decreases the velocity of the propagation of the current.

(2) The effect of the parameter Π is opposite: as Π increases, the current propagates faster. For $\Pi \gg 1$, the effect of stratification becomes insignificant as compared with the driving force of the particles.

(3) For the currents propagating into a nonstratified ambient, for any degree of the polydispersity, the current propagates faster than the equivalent monodisperse current with an average settling velocity, but the discrepancy between them is insignificant.

(4) For $\Pi \approx \frac{1}{S}(1 - \frac{1}{2H})$, the current is expected to behave like a homogeneous current spreading in a nonstratified ambient.

An additional simplified box model was developed for the containers of general CSs. We solved this model numerically and compared with the results of the SW model. In general, the box model underestimates the distance of propagation of the current, x_N, by 10–20 %.

Overall, this work provides a major extension and generalization of the theory of monodisperse currents propagating into a stratified ambient in containers of general forms to polydisperse currents in the same environment (see Ref. [15]). The current becomes homogeneous for $\Pi = 0$ and the ambient becomes nonstratified for $S \to 0$ or $\Pi \gg 1$.

More investigation is still needed to further assess the accuracy of the entrainment and drag closures needed in the extended SW model. This requires careful comparisons with more experimental data. An additional interesting direction is the study by Navier-Stokes simulation, which might point out details of the motion and must be left for future work.

ACKNOWLEDGMENT

APPENDIX: REDUCING OF GOVERNING EQUATIONS TO SYSTEM OF THREE EQUATIONS ONLY

In this section we follow the approach presented by Zemach [11]. We start with the equations of motion: the first two equations are the conservation and momentum equations; the last n equations are the mass concentration equations written for each kind of the particle:

$$\frac{\partial A}{\partial t} + \frac{\partial (Au)}{\partial x} = 0,$$
$$\frac{\partial (Au)}{\partial t} + \frac{\partial (Au^2)}{\partial x} + \frac{\partial A}{\partial x}\frac{A}{f(h)}\left[\Pi\Phi + 1 - S\left(1 - \frac{h}{H}\right)\right] + \Pi\frac{\partial \Phi}{\partial x}A\Psi(h) = 0,$$
$$\frac{\partial (A\phi^{(j)})}{\partial t} + \frac{\partial (Au\phi^{(j)})}{\partial x} = -\beta^{(j)}\phi^{(j)}f_M, \quad \text{for} \quad j = 1, 2, \ldots, n. \tag{A1}$$

The last n equations of system (A1) can be rewritten in the following form:

$$\frac{d\phi^{(j)}}{dt} = -\beta^{(j)}\phi^{(j)}h\frac{f_M(h)}{A(h)}, \quad j = 1, 2, \ldots, n. \tag{A2}$$

A closer look at these n equations provides a conclusion that, once the model is solved for some virtual $\phi^{(0)}(x, t)$ with $\phi_0^{(0)}$ and $\beta^{(0)}$, the other $\phi^{(j)}$ will follow simply for any $j = 1, 2, \ldots, n$:

$$\phi^{(j)}(x, t) = \phi_0^{(j)} \left[\frac{\phi^{(0)}(x, t)}{\phi_0^{(0)}} \right]^{\frac{\beta^{(j)}}{\beta^{(0)}}}. \tag{A3}$$

This suggests the following substitution:

$$\phi^{(j)}(x, t) = \phi_0^{(j)} e^{\beta^{(j)} G(x, t)}, \tag{A4}$$

initially $G(x, 0) = 0$. The substitution of Eq. (A4) into the last n equations of Eqs. (A1) reduces these n equation to the same equation for $G(x, t)$:

$$\frac{\partial (AG)}{\partial t} + \frac{\partial (AGu)}{\partial x} = -f_M. \tag{A5}$$

[1] S. Hsu, J. Kuo, C. Lo, C. Tsai, W. Doo, C. Ku, and C. Sibuet, Turbidity currents, submarine landslides and the 2006 Pingtung earthquake off SW Taiwan, Terr. Atmos. Ocean. Sci. **19**, 767 (2008).

[2] R. T. Bonnecaze, H. E. Huppert, and J. R. Lister, Particle-driven gravity currents, J. Fluid Mech. **250**, 339 (1993).

[3] T. Maxworthy, J. Leilich, J. E. Simpson, and E. H. Meiburg, The propagation of gravity currents in a linearly stratified fluid, J. Fluid Mech. **453**, 371 (2002).

[4] Z. He, L. Zhao, J. Chen, C. Yu, and E. Meiburg, Particle-laden gravity currents interacting with stratified ambient water using direct numerical simulations, Environ. Earth Sci. **80**, 732 (2021).

[5] C. A. Mériaux and C. B. Kurz-Besson, Sedimentation from binary suspensions in a turbulent gravity current along a V-shaped valley, J. Fluid Mech. **712**, 624 (2012).

[6] C. A. Mériaux and C. B. Kurz-Besson, A study of gravity currents carrying polydisperse particles along a V-shaped valley, Eur. J. Mech. B Fluids **63**, 52 (2017).

[7] C. Gladstone, J. C. Philips, and R. S. J. Sparks, Experiments on bidisperse, constant-volume gravity currents: Propagation and sediment deposition, Sedimentology **45**, 833 (1998).

[8] T. H. Harris, A. G. Hogg, and H. E. Huppert, Polydisperse particle-driven gravity currents, J. Fluid Mech. **472**, 333 (2002).

[9] M. M. Nasr-Azadani, B. Hall, and E. Meiburg, Polydisperse turbidity currents propagating over complex topography: Comparison of experimental and depth-resolved simulation results, Comput. Geosci. **53**, 141 (2013).

[10] T. Zemach, Particle-driven gravity currents in non-rectangular cross-section channels, Phys. Fluids **27**, 103303 (2015).

[11] T. Zemach, Polydisperse particle-driven gravity currents in non-rectangular cross section channels, Phys. Fluids **30**, 016601 (2018).

[12] T. Zemach, L. Chiapponi, D. Petrolo, M. Ungarish, S. Longo, and V. Di Federico, On the propagation of particulate gravity currents in circular and semi-circular channels filled with homogeneous or stratified ambient fluid, Phys. Fluids **29**, 106605 (2017).

[13] T. Zemach and M. Ungarish, Gravity currents in non-rectangular cross-section channels: Analytical and numerical solutions of the one-layer shallow-water model for high Reynolds-number propagation, Phys. Fluids **25**, 026601 (2013).

[14] W. B. Dade and H. E. Huppert, A box model for non-entraining suspension-driven gravity surges on horizontal surfaces, Sedimentology **42**, 453 (1995).

[15] M. Ungarish, *Gravity Currents and Intrusions: Analysis and Prediction* (World Scientific, Singapore, 2020).

[16] M. Ungarish, Shallow-water solutions for gravity currents in non-rectangular cross-area channels with stratified ambient, Environ. Fluid Mech. **15**, 793 (2015).

[17] M. Ungarish, A general solution of Benjamin-type gravity current in a channel of non-rectangular cross-section, Environ. Fluid Mech. **12**, 251 (2012).

[18] M. Ungarish, *An Introduction to Gravity Currents and Intrusions* (CRC Press, Boca Raton, FL, 2009).

[19] A. G. Hogg, M. Ungarish, and H. Huppert, Particle-driven gravity currents: Asymptotic and box model solutions, Eur. J. Mech. B Fluids **19**, 139 (2000).

[20] T. Zemach, Asymptotic similarity solutions for particle-driven gravity currents in non-rectangular cross-section channels of power-law form, Eur. J. Mech. B Fluids **74**, 312 (2019).

[21] J. J. Monaghan, C. A. Mériaux, H. E. Huppert, and J. Mansour, Particulate gravity currents along V-shaped valleys, J. Fluid Mech. **631**, 419 (2009).